

# Polymer solar cell modules prepared using roll-to-roll methods: Knife-over-edge coating, slot-die coating and screen printing

Frederik C. Krebs

Risø National Laboratory for Sustainable Energy, Technical University of Denmark, Frederiksborgvej 399, DK-4000 Roskilde, Denmark

## ARTICLE INFO

### Article history:

Received 30 September 2008  
Received in revised form  
4 December 2008  
Accepted 9 December 2008  
Available online 21 January 2009

### Keywords:

Polymer solar cells  
Thermocleavable materials  
P3MHOCT  
P3CT  
P3HT-PCBM  
Production  
Fabrication  
Roll-to-roll (R2R) coating  
Knife-over-edge coating  
Slot-die coating  
Screen printing  
Modules  
Ambient processing  
Solution processing

## ABSTRACT

A complete polymer solar cell module prepared in the ambient atmosphere using all-solution processing with no vacuum steps and full roll-to-roll (R2R) processing is presented. The modules comprise five layers that were prepared on a 175- $\mu\text{m}$  flexible polyethyleneterephthalate (PET) substrate with an 80-nm layer of transparent conducting indium–tin oxide (ITO). The ITO layer was first patterned by screen printing an etch resist followed by etching. The second layer was applied by either knife-over-edge (KOE) coating or slot-die coating a solution of zinc oxide nanoparticles (ZnO-nps) followed by curing. The second layer comprised a mixture of the thermocleavable poly-(3-(2-methylhexan-2-yl)-oxy-carbonyldithiophene) (P3MHOCT) and ZnO-nps and was applied by a modified slot-die coating procedure, enabling slow coating speeds with low viscosity and low surface tension ink solutions. The third layer was patterned into stripes and juxtaposed with the ITO layer. The fourth layer comprised screen-printed or slot-die-coated PEDOT:PSS and the fifth and the final layer comprised a screen-printed or slot-die-coated silver electrode. The final module dimensions were 28 cm  $\times$  32 cm and presented four individual solar cell modules: a single-stripe cell, a two-stripe serially connected module, a three-stripe serially connected module and finally an eight-stripe serially connected module. The length of the individual stripes was 25 cm and the width was 0.9 cm. With overlaps of the individual layers this gave a width of the active layer of 0.6 cm and an active area for each stripe of 15 cm<sup>2</sup>. The performance was increased ten fold compared to mass-produced modules employing screen printing for all five layers of the device. The processing speeds employed for the R2R processed layers were in the range of 40–50 m h<sup>-1</sup>. Finally a comparison is made with the state of the art represented by P3HT-PCBM as the active layer and full R2R solution processing using slot-die coating.

© 2009 Elsevier B.V. All rights reserved.

## 1. Introduction

One of the advantages that polymer solar cells have to offer over all photovoltaic technologies is the alleged possibility to process them, in large area on flexible substrates [1,2], entirely from solution by printing and coating techniques [3,4], without indium–tin oxide (ITO) [5,6], at low temperature, with no need for vacuum coating steps. The current status is however far from this vision and to this date most reports on polymer solar cells is for devices with a very small active area ( $\ll 1 \text{ cm}^2$ ) on glass-ITO substrates. In addition, the film-forming technique that is used almost exclusively is spin coating and most often the devices comprise one or two vacuum-coated layers. The focus of the research has been on achieving as high power conversion efficiency (PCE) as possible and the state of the art today is around 6.5% for a tandem device [7]. The equally important areas of operational stability, degradation and processing techniques

have been sadly neglected and if polymer solar cells are to become more than a scientific curiosity that enjoyed popularity at the turn of the millennium these points must be addressed convincingly. The field of polymer photovoltaics has been reviewed numerous times and addressed from different angles. Some of the most recent reviews address new low-band-gap materials, stability, degradation and morphology [8–12]. In order to process polymer solar cells in high volume and large area there is no doubt that the methodology will have to involve roll-to-roll (R2R)-compatible techniques and it is most likely that the printing or coating technique will also be required to have the capacity to pattern the printed or coated layer. It is thus somewhat ironic that the experimental method of choice is spin coating, which is not inherently R2R compatible and does not allow for patterning of the film. This possibly implies that the majority of processing knowledge developed so far (on spin coating) is not directly usable or transferable to an industrially relevant process. This knowledge will then have to be developed separately. The use of spin coating is a highly valuable technique for materials screening and laboratory work but one should exercise care when

E-mail address: [frederik.krebs@risoe.dk](mailto:frederik.krebs@risoe.dk)

extrapolating results from spin-coated laboratory cells and using these for projecting marvels of the technology in terms of performance and cost.

In this manuscript I detail experiments with R2R processing of complete polymer solar cell modules on a reasonable scale. Several different processing techniques are employed and the results are discussed in the context of the developments that are needed. An additional aim of this work was to compare the performance that could be obtained for a known materials combination and device geometry simply by changing the processing techniques employed for fabrication.

## 2. Experimental

### 2.1. General materials

Zinc oxide nanoparticles (ZnO-nps) were prepared and stabilised with methoxyethoxyacetic acid (MEA) as described earlier [13]. Poly-(3-(2-methylhexan-2-yl)-oxy-carbonyldithiophene) (P3MHOCT) has been employed in an experiment with large-scale production and was obtained and purified in the same manner ( $M_n = 11,300$ ,  $M_w = 36,900$ ,  $M_p = 29,800$ ,  $PD = 3.3$ ) [3,14]. The thermocleavable solvent WS-1 has been patented and its use for printing solar cells described [3,15,16]. PEDOT:PSS was purchased as a screen-printing paste from Agfa (Orgacon EL-P 5010, [www.agfa.com](http://www.agfa.com)). The silver electrode was purchased from Dupont as a screen-printing paste (Dupont 5007, [www.dupont.com](http://www.dupont.com)). P3HT was prepared according to the McCollough route [17] and was purified by removal of metal salts and through multiple Soxhlet extraction cycles ( $M_n = 18,700$ ,  $M_w = 36,600$ ,  $M_p = 33,900$ ,  $PD = 1.9$ ). [60]PCBM was obtained from Solenne BV.

### 2.2. R2R coating system

The system employed in this study is a commercially available Basecoater (BC30 from solar coating machinery, Germany, [www.solarcoating.de](http://www.solarcoating.de)) as shown in Fig. 1, which has been modified for the purpose of these experiments. The machine comprises an unwinder, corona treater (Arcotec), air knife static discharger, coating unit, hot-air dryer, cooling roller and rewinder. In addition, the system is equipped with four video cameras, enabling online monitoring and control of the process. A total of three humidity sensors are positioned: one each in the coating chamber, for the air entering the heater on the oven and in the room where the instrument is placed. The coating was done under tension control with the coating roller as the driver for the web. The winding and unwinding unit operated with a tension on the web of around 100 N.

The roll width on the system is 300 mm with a working width of 250 mm. The substrate width was practically chosen to be 280 mm in order to avoid problems with misalignment during coating (no edge guiding system was implemented during these experiments).

### 2.3. Pattern

The pattern was chosen to enable the preparation of a single cell and also serially connected cells. In addition to a single line (for the single cell), two, three and eight cells were also included for testing serial connection in small modules. For this purpose two different patterns were required. The first pattern comprised the stripes that were applied for the ITO layer, the active layer and the PEDOT:PSS layer. The second pattern comprised contact lines for extraction of the electrical current and was employed for the silver back electrode as shown in Fig. 2. The ZnO-np layer was

either coated evenly over the substrate surface in which case no pattern was necessary or patterned according to the ITO layer.

The margin employed for the overlaps and interconnects was large to ensure ease during processing. In practical terms this implies that a relatively large aperture loss of  $>50\%$  was obtained (this can be optimised in a later process where a reduction of the aperture loss to 20% is estimated to be possible).

### 2.4. Processing of the ITO

The substrate was purchased as ITO-covered poly(ethylene terephthalate) (PET; 175  $\mu\text{m}$ ) in rolls having a roll width of 305 mm and a length of 100 m. The material was used as received from Innovative Specialty Films (ISF, T-MOX). The nominal sheet resistance was  $60 \Omega \text{square}^{-1}$ . The material was trimmed to a web width of 280 mm and reference holes were punched along the edges. The desired striped pattern of the ITO was prepared by printing a UV-curable etch resist in the areas of the ITO pattern on a Klemm line in a full R2R process. The printing speed was  $180 \text{prints h}^{-1}$ . The pattern is shown to the left in Fig. 2 and comprises stripes with a width of 9 mm and a length of 250 mm along the direction of the web. The repetition distance was 275 mm since it is not possible to print continuous lines with a reversing screen printer. The distance of 25 mm between the stripes in the length direction allowed for a sufficient margin between prints. The processing speed for printing and UV curing the etch resist was thus  $49.5 \text{m h}^{-1}$ . The ITO was subsequently etched using a full R2R etching machine comprising etching baths ( $\text{CuCl}_2$ ), stripping baths (NaOH), washing baths (demineralised water) and drying sections (hot air). The etching speed was  $40 \text{m h}^{-1}$ . The thickness of the ITO was 80 nm.

### 2.5. Knife-over-edge coating of the ZnO layer

The ZnO-np ink was prepared by stabilising ZnO-nps with MEA in WS-1 solvent at a concentration of ZnO-nps of  $50 \text{mg mL}^{-1}$  (the MEA concentration was  $10 \text{mg mL}^{-1}$ ). This stock solution was quite stable in time. Prior to coating, the stock solution was diluted with four volumes of ortho-xylene, giving a total ZnO-np concentration of  $10 \text{mg mL}^{-1}$  in the final ink. The solution was filtered through a 0.45- $\mu\text{m}$  Teflon filter and used directly for coating. The temperature and relative humidity during coating were, respectively,  $23 \pm 3^\circ\text{C}$  and  $55 \pm 2\%$ . The web speed was set to  $0.8 \text{m min}^{-1}$  and the ink was fed manually in front of the knife. The gap was 0.3 mm and the tension on the web was 100 N. The temperature of the hot air entering the oven was  $150^\circ\text{C}$ . The measured temperatures in the oven (in eight places) were in the range  $125\text{--}130^\circ\text{C}$ . With an oven length of 1 m the drying time was 75 s. The cooling roller was operated at  $16^\circ\text{C}$ . The final processed PET/ITO/ZnO substrate was kept in the room at a relative humidity of  $50 \pm 7\%$  on the rewinder for 16 h, during which period of time the ZnO-nps react further with humidity from the atmosphere, giving a completely insoluble layer (in organic solvents). A 25 mL portion of ink allowed for the coating of 45–47 modules. There is little or no loss involved and all modules were typically usable (sometimes the first and last module where only partially coated). The thickness of the layer was  $20 \pm 10 \text{nm}$  and quite uneven.

### 2.6. Slot-die coating of the ZnO-np layer

The ink for slot-die coating of ZnO-nps was prepared by mixing a MEA (20%) stabilised stock solution of ZnO-nps ( $4 \text{mL}$ ,  $130 \text{mg mL}^{-1}$ ) in chlorobenzene with ortho-xylene ( $6 \text{mL}$ ) and WS-1 ( $1 \text{mL}$ ). The solution was filtered through a 0.45- $\mu\text{m}$  Teflon filter and used directly for coating. The temperature and relative

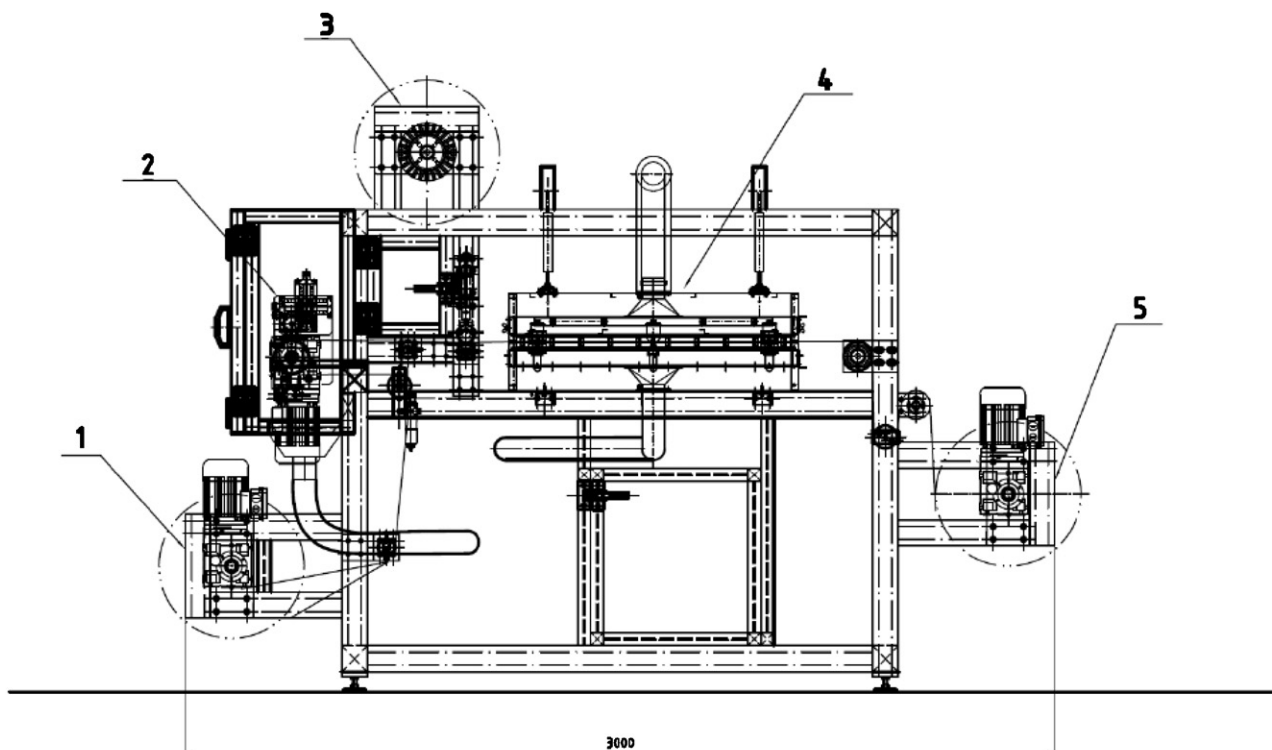


**Fig. 1.** Schematic of the coating machine comprising: (1) unwinder, (2) coating chamber, (3) lamination station, (4) hot-air oven and (5) rewinder. The total length of the unit is 3 m (top). Photographs of the coating system (left) and the monitoring during coating are also shown (right).

humidity during coating were, respectively,  $23 \pm 3$  °C and  $48 \pm 2$ %. The web speed was set to  $0.8 \text{ m min}^{-1}$  and the ink was fed into the slot-die coating head. The web tension, oven and cooling roller temperatures, and repository time were the same as in Section 2.5. The slot-die coating head was modified with a meniscus guide to enable good control of the meniscus during coating. The slot-die coating head was adjusted in a direction orthogonal to the web direction such that the coated pattern was shifted 1 mm with respect to the ITO pattern. The ITO and the coated lines had a width of 9 mm and the overlap was thereby 8 mm. The thickness of the layer was  $60 \pm 10$  nm and uneven areas were observed due to reaction with humidity prior to drying.

### 2.7. Slot-die coating the active layer and thermocleavage

The ink for the active layer was prepared by dissolving 280 mg of P3MHOCT in ortho-xylene (6 mL) at 70 °C with gentle stirring;

0.025 mL MEA was added to this solution followed by a ZnO-np solution in chlorobenzene ( $130 \text{ mg mL}^{-1}$ ) stabilised with MEA ( $6.5 \text{ mg mL}^{-1} \sim 5\%$  w/w). The total volume after mixing was 10 mL and the total MEA content was 10% (w/w) with respect to zinc oxide. The solution was filtered through a 0.45- $\mu\text{m}$  Teflon filter and used directly for coating. The temperature and relative humidity during coating were, respectively,  $23 \pm 3$  °C and  $48 \pm 2$ %. The web speed was set to  $0.8 \text{ m min}^{-1}$  and the ink was fed into the slot-die coating head. The web tension, and oven and cooling roller temperatures were the same as in Section 2.5. The slot-die coating head was modified with a meniscus catcher to enable good control of the meniscus during coating. The slot-die coating head was adjusted in a direction orthogonal to the web direction such that the coated pattern was shifted 2 mm with respect to the ITO pattern. The ITO and the coated lines had a width of 9 mm and the overlap was thereby 7 mm. After coating and drying, the material was cut into sheets and thermocleaved in a hot-air oven for 140 °C for 4 h. The lot of 10 mL of ink typically

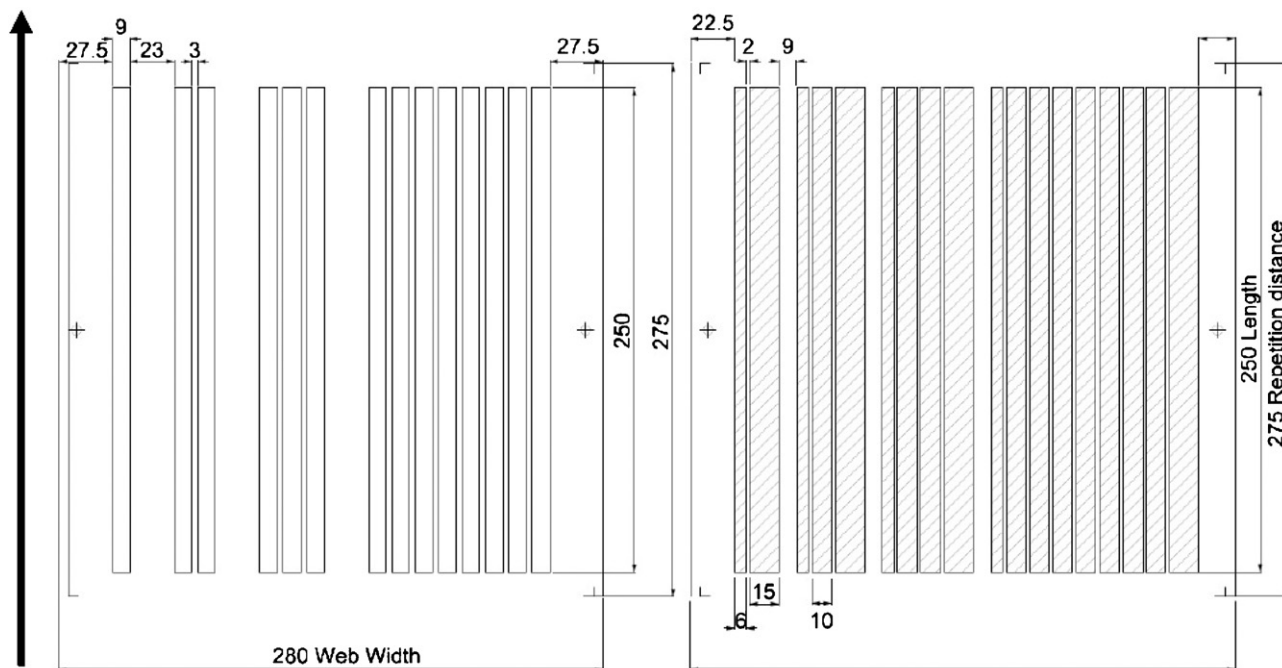


Fig. 2. Drawing of the two patterns employed for preparing the modules. The pattern employed for ITO, the active layer and PEDOT:PSS (left) and the silver back electrode (right). The direction of the web is indicated by an arrow.

gave 20–30 coated modules of which 15–25 were coated without error. The initial modules have errors since not all menisci are pinned at the same time and it takes a little while to adjust the pattern so that it matches the ITO pattern with the required difference of 1 mm. The assembly of the slot-die coating head with the mask for the active layer is shown in Fig. 3. After coating and drying, the material was cut manually into sheets, one sheet for each module. The sheets were placed in a hot-air oven at 140 °C for 4 h to thermocleave the active layer and achieve insolubility. The thickness of the active layer was  $250 \pm 30$  nm. The ink solution for slot-die coating of P3HT-PCBM comprised  $22 \text{ mg mL}^{-1}$  P3HT and  $20 \text{ mg mL}^{-1}$  PCBM in a 1:1 mixture of 1,2-dichlorobenzene and chloroform. The coating procedure was the same as above.

#### 2.8. Screen printing and slot-die coating of the PEDOT:PSS layer and silver back electrode

After thermocleavage the guide holes were punched along the edge of the substrate closest to the single stripe in order to enable registration of the screen-printing mask and the substrate. PEDOT:PSS (Orgacon EL-P 5010) was then screen printed on top of the structure with the pattern shifted 1 mm to the side with respect to the active layer and 3 mm with respect to the ITO pattern. The PEDOT:PSS was printed using a 165 mesh screen with the same pattern as the ITO using a printing speed of  $525 \text{ mm s}^{-1}$ . After printing, the sheets were dried at 130 °C for 15 min in a hot-air oven. The typical sheet resistivity was  $200\text{--}300 \Omega \text{ square}^{-1}$ . The Dupont 5007 silver back electrode was screen printed through a 120 mesh mask on top of the PEDOT:PSS layer with the pattern shifted slightly 0.3–6 mm to the side with respect to the active layer and dried at 130 °C for 3 min. The typical sheet resistivity was  $0.03\text{--}0.1 \Omega \text{ square}^{-1}$ . The total overlap of ITO and PEDOT:PSS–silver electrodes is  $\sim 6$  mm. When slot-die coating the PEDOT:PSS on top of the active layers it was found necessary to dilute the PEDOT:PSS with isopropanol to give a viscosity of  $\sim 200 \text{ mPa s}$  (100 g Agfa 5010 was mixed by thorough shaking with 60 g isopropanol). When slot-die coating the Dupont 5007 it was found necessary to dilute the ink with a thinner to a viscosity of

$\sim 200 \text{ mPa s}$ . It is essential to use a 100- $\mu\text{m}$  mask in the coating head and to avoid clogging. The time between printing and drying has to be as fast as possible in the case where P3HT-PCBM is used as the active layer as the solvents in the silver ink destroys the active layer on prolonged exposure (the time to drying must be less than 1 min).

#### 2.9. Module characterisation

The effective active area for each stripe is typically  $250 \text{ mm} \times 6 \text{ mm}$ . The width varies a little depending on the alignment and therefore the overlap between the ITO electrode and the PEDOT:PSS–silver back electrode also varies. The nominal active areas, aperture areas and geometric fill factor for the modules were as follows: single-stripe modules ( $15 \text{ cm}^2$ ,  $57.5 \text{ cm}^2$ , 26%), two-stripe module ( $30 \text{ cm}^2$ ,  $87.5 \text{ cm}^2$ , 34%), three-stripe module ( $45 \text{ cm}^2$ ,  $117.5 \text{ cm}^2$ , 38%) and the eight-stripe module ( $120 \text{ cm}^2$ ,  $267.5 \text{ cm}^2$ , 45%). The  $I$ - $V$  characteristics were recorded using a Keithley 2400 sourcemeter. The conditions of the characterisation under simulated sunlight were KHS 575 solar simulators from Steuernagel Lichttechnik operating at  $1000 \text{ W m}^{-2}$ , AM1.5G,  $45 \pm 5\%$  relative humidity and  $72 \pm 3$  °C. The spectrum of the solar simulator was checked using an optical spectrum analyser calculated for measuring irradiance. The incident light intensity of the solar simulator was calibrated bolometrically using a precision spectral pyranometer from Eppley Laboratories ([www.eppleylab.com](http://www.eppleylab.com)). The incident light intensity was monitored continuously during measurements using a CM4 high-temperature pyranometer from Kipp & Zonen ([www.kippzonen.com](http://www.kippzonen.com)).

### 3. Results and discussion

#### 3.1. Choice of device type

Polymer solar cell devices are most practically developed in the laboratory on a small scale using spin coating. In the majority of cases this exercise serves the purpose of evaluating the

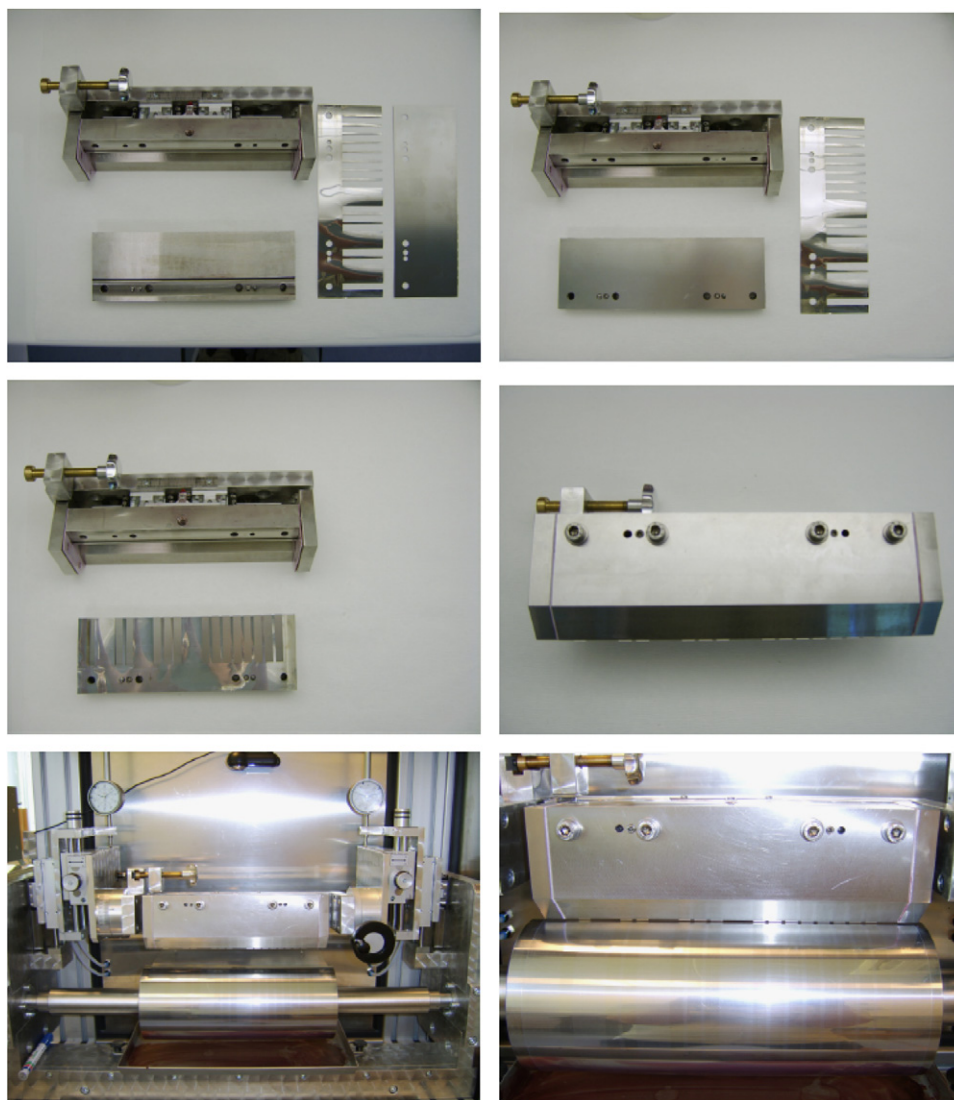


**Fig. 3.** Assembly of the slot-die coating head, insertion into the coating chamber and positioning over the web on the coating roller. The four parts (top left), the meniscus guide mask is positioned on top of the front wedge of the die (top right), the slot-die mask is positioned on top of the meniscus catcher (middle left), the slot-die coating head is assembled (middle right), the slot-die coating head is fastened over the coating roller (bottom left) and finally the coating head is positioned with respect to the ITO pattern (bottom right). The ITO is visible as stripes.

performance of new materials or device architectures and there is rarely a need to extend beyond the laboratory level. In many instances the experimenter accepts some practicalities related to the material and device type in question that can be dealt with on the laboratory scale but they become prohibitive when wishing to extend beyond the laboratory scale (to a larger scale).

A current belief is that the future of polymer solar cell production lies within the confines of the coating and printing industry and that the machinery that will be employed are coating and printing machines. It may thus seem trivial to transfer a laboratory device to a larger scale by using different film-forming equipments but in actual fact this poses severe challenges. The purpose of this work was to attempt this and describe the effort and challenges that one is faced with and also provide some of the solutions to the problems without which transfer from laboratory to a R2R process is not possible. In order to minimize the number of problems that has to be overcome, the choices of solar cell geometry, device structure and materials are important. Firstly, the materials have to be stable under the processing conditions that due to the physical size of the experiment are necessarily in

the ambient atmosphere. It would also be required that the final device be stable with respect to photovoltaic properties on storage and handling in air and to a certain extent also during operation. The device structure has to be as simple as possible with as small a requirement as possible on the film-forming techniques. Finally, the substrate has to be flexible and readily adaptable to a R2R process. The choice of substrate fell on commercially available 175- $\mu\text{m}$  thick PET foil with a layer of ITO. The choice of polymer technology was the thermocleavable P3MHOCT as a bulk hetero-junction with ZnO-nps as this type of device has been shown to have good operational stability in air [4] and to be processable in air [3,13] without the need for vacuum coating steps.

### 3.2. Choice of device geometry

Since the ITO on the PET substrate has a nominal sheet resistance of  $60\ \Omega\ \text{square}^{-1}$  the size of the individual cells has to be kept small in order to minimize sheet resistive losses in the ITO electrode. The back electrode is a silver paste electrode with a

much lower sheet resistivity that is typically  $<0.1 \Omega \text{square}^{-1}$ . The device structure was thus made to accommodate this such that as little of the charge transport is through the ITO and as much as possible through the silver electrode. It was also of some interest to establish if a serial connection between many cells was readily adaptable to a R2R process and for this reason the processed solar cell sheet contained both a single cell and various serially connected modules. The device outline is shown in Fig. 4 for a module comprising two serially connected cells processed in two different ways. The device structure generally applied for both the single cell and the other serially connected modules. By printing extra silver lines at the ends of the module, extraction of the electrical current was made as efficient as possible with minimal resistive loss.

### 3.3. R2R processing of the layers

The aim was to process as many of the layers by R2R methods without vacuum steps starting from a commercially available substrate material. The serial connection of cells in the module required that the transparent conductor (ITO) was patterned into stripes. The striped pattern was created by R2R screen printing an etch resist of the stripes. The Klemm line employs a reversing flat screen and it is thus not possible to prepare continuous stripes and instead a small break in the striped pattern was employed such that the stripes were 250 mm in length along the direction of the web separated by 25 mm. The repetition distance of the ITO pattern along the direction of the web was 275 mm. After printing of the etch resist the unmasked ITO was etched using a R2R etching bath followed by stripping of the etch resist, washing and drying of the substrate. This PET substrate with the patterned ITO was the substrate for the remaining steps in the process. The PET-ITO substrate was transferred to the laboratory coater shown in Fig. 1. A layer of ZnO-nps was then either coated evenly over the entire surface of the PET-ITO using knife-over-edge (KOE) coating or patterned into stripes using slot-die coating. It is in principle not necessary to pattern the ZnO into stripes. The ZnO layer acts as a hole-blocking electron-transporting layer and forms an excellent contact with both ITO and silver. There is thus in principle a very small loss in the ITO-ZnO-Ag junction, which is Ohmic. The simplicity of coating an even coat over the entire surface is so attractive that this route was also pursued. In addition, slot-die coating was also attempted in separate experiments. The problem with ZnO-np solutions is their sensitivity to humidity from the

atmosphere and as shown earlier it is possible to stabilise the solution with MEA, which slows the reaction down but also makes the drying and crosslinking time longer. Unstabilised ZnO-nps can be processed into a film with a high optical quality only under anhydrous conditions in a glovebox and form an insoluble (crosslinked) film on heating briefly to  $200^\circ\text{C}$  or by exposure to the atmosphere (humidity). When stabilising the ZnO-nps it becomes possible to process films of a good optical quality in the ambient atmosphere but in order to achieve insolubility of the film, heating to higher temperatures for longer periods of time or much longer repository times are needed. This was explored in a work where the ZnO layer was screen printed whereby the film was dried at the maximum temperature that PET will endure ( $\sim 140^\circ\text{C}$ ) for 2 h followed by a long repository time of 16 h. The insolubility is essential for device function since processing of the subsequent layers must not dissolve or affect the ZnO layer. From this point of view a substrate that can endure a higher temperature (i.e.  $210\text{--}300^\circ\text{C}$ ) would be desirable. There are few polymer materials that can handle this (i.e. Kapton). The ink for the ZnO layer was thus prepared by MEA stabilisation and it was found beneficial to include around 20% (w/w) of the thermocleavable solvent WS-1 in the ink mixture.

KOE coating proceeded smoothly with drying at  $140^\circ\text{C}$ . The ZnO film was insoluble after 16 h of reposing in the ambient atmosphere with a relative humidity of  $50 \pm 7\%$ . There is no humidity control in the room housing the coating equipment and it was found that the ZnO layer was best processed on days with a lower humidity. The material was rewound and the active layer was applied by slot-die coating. The viscosity of the ink solution is around  $1 \text{ mPa}\cdot\text{s}$  and since the coating speed is quite slow (technically limited to  $\leq 2 \text{ m}\cdot\text{min}^{-1}$ ) it was found very difficult to control the menisci during slot-die coating such that the coated stripes of active materials were positioned correctly with respect to ITO (1-mm offset lines). Some experimentation on the ink composition was made and it was found desirable to employ a mixture of chlorobenzene and ortho-xylene containing a little of the thermocleavable solvent WS-1. It was possible to use traditional slot-die coating at the speeds employed ( $0.7\text{--}0.9 \text{ m}\cdot\text{min}^{-1}$ ) but it was very difficult to control all the menisci at the same time and many errors were introduced with overlapping stripes. In order to efficiently solve this, an extra mask was prepared that helped to pin or guide the meniscus in front of each slot that was included in front of the mask defining the slots when assembling the slot-die coating head as shown in Fig. 3. The extra mask has a small protrusion in front of the slot, which helps in the

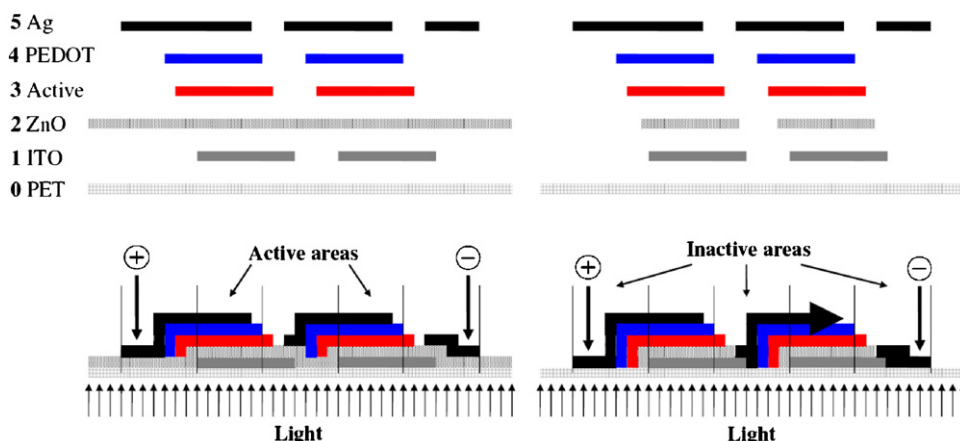
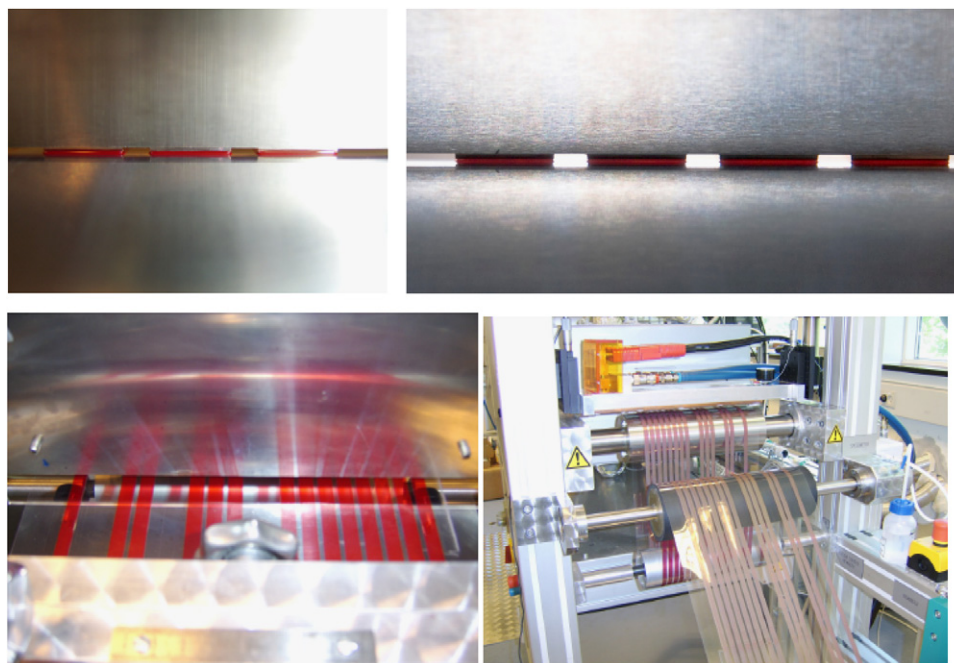
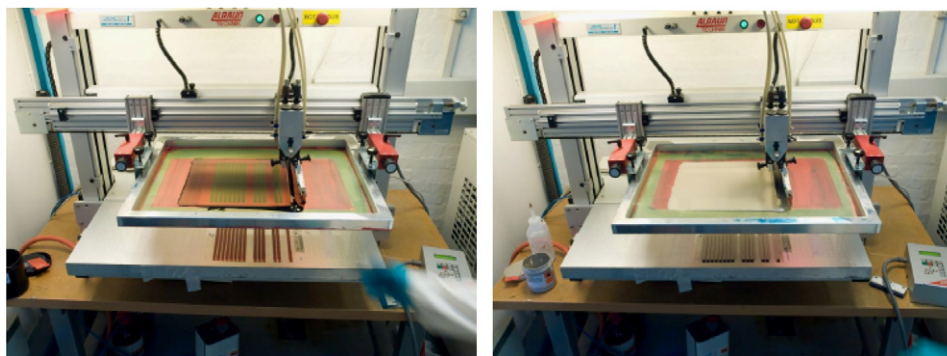


Fig. 4. Exploded views of the device structure for a module comprising two serially connected cells prepared by knife-over-edge coating ZnO nanoparticles (left) or slot-die coating (right). The layer sequence on the PET substrate is also shown (above) and a schematic cross-section (not to scale) of the final device with the overlap of layers, aperture loss and active area (below).



**Fig. 5.** Close-up view of the meniscus as seen with front illumination (top left) and back side illumination (top right). The wet film shown just behind the slot-die coating head (bottom left) and the dried film on the rewinding side (bottom right).



**Fig. 6.** Screen printing of the PEDOT:PSS (left) and the silver electrode (right) layer using a manually fed screen printer.

pinning of the meniscus below the slot and prevents the menisci between two adjacent lines from joining (3 mm distance) as shown with front and rear illumination in Fig. 5. This method is to my knowledge novel and can be viewed as a combination of slot-die and slide coating. Without this development, coating of the inks prepared here would be near impossible at the slow speeds employed. This made coating and adjustment very easy. The wet-coated film was then dried in the hot-air oven close to the maximum possible temperature of 140 °C (see wet and dry films in Fig. 5). Since the oven length is only 1 m the drying time at the speeds employed was around 1 min. This drying time is much too short to achieve thermocleavage of P3MHOCT to P3CT, which is required before the PEDOT:PSS and silver layers can be applied. Future work will have to solve the temperature limitation of the substrate (i.e. PET) by either (1) finding an alternative substrate that supports high temperature (>210 °C) or (2) by development of different materials that allow for the insolubility switching in the temperature range that PET supports or finally by (3) development of an alternative method for carrying out thermocleavage. In order to thermocleave P3MHOCT to P3CT, two approaches were attempted: either by heating the wound roll in an oven at 140 °C until insolubility was reached or by cutting the

coated material into sheets with the individual modules and then heating the sheets in an oven at 140 °C until insolubility was reached. The former approach was problematic due to the thermal expansion of the material resulting in defects in the coated films due to the expansion contraction on the roll leading to friction between layers. The latter approach was followed and the material was cut into sheets and thermocleaved in a hot-air oven at 140 °C for 4 h. Holes were then punched along the side, allowing for positioning the sheets with respect to the screen-printing mask. PEDOT:PSS was then screen printed on top of the active layer and dried in an oven at 130 °C for 15 min. Silver paste electrodes were finally screen printed on top of the entire structure to complete the device as shown in Fig. 6. A clear limitation is that the last two layers (PEDOT:PSS and silver) were not processed by a R2R process. It should however be emphasized that the problem was not linked to the PEDOT:PSS and silver layers but rather to the temperature required for thermocleavage, which was not reasonably achievable in a R2R process (i.e. several hours at 140 °C). Both PEDOT:PSS and silver could have been readily transferred to a R2R process using the Klemm R2R screen-printing line that was used for the patterning of ITO.

The methods employed are all R2R compatible and the processing speeds employed here have been summarized in Table 1. While both the PEDOT:PSS and silver electrodes were prepared by sheet-fed screen printing the processing speed that

can be anticipated is similar to the application of the etch resist ( $49.5 \text{ m h}^{-1}$ ).

### 3.4. Surface roughness of the individual layers

When preparing multilayer structures the smoothness of the layers is of some importance as each coated layer (except the last layer) will serve as the coating surface of the subsequent layer. For thick coating inks with good levelling properties it is generally possible to even out a roughness in the previous coat as the solid content in the ink is high and the wet thickness is thereby not too different from the dry film thickness. For inks employed in polymer photovoltaics the solids content is generally quite low and the dry thickness is much thinner than the wet film thickness. This implies that defects and protrusions are reproduced and perhaps amplified in subsequent layers. In order to address this, AFM images (Fig. 7) were recorded for all the surfaces used and prepared here. The PET and ITO surfaces are quite smooth with variations in topography in the range of 0–30 nm over a  $5 \times 5 \mu\text{m}^2$  area. The ZnO surface was also quite smooth with distinct

**Table 1**  
Processing speeds employed here for all the individual coating steps.

Step	Processing technique	Type	Processing speed ( $\text{m h}^{-1}$ )
Application of resist	Screen printing	R2R	49.5
Etching and stripping	Bath etching	R2R	40.0
ZnO-np layer	Knife over edge	R2R	48.0
Active layer	Slot die	R2R	48.0
PEDOT:PSS	Screen printing	Manual	–
PEDOT:PSS <sup>a</sup>	Slot die	R2R	12.0
Ag back electrode	Screen printing	Manual	–
Ag back electrode <sup>a</sup>	Slot die	R2R	60.0

<sup>a</sup> P3HT-PCBM modules processed entirely from solution using slot-die coating.

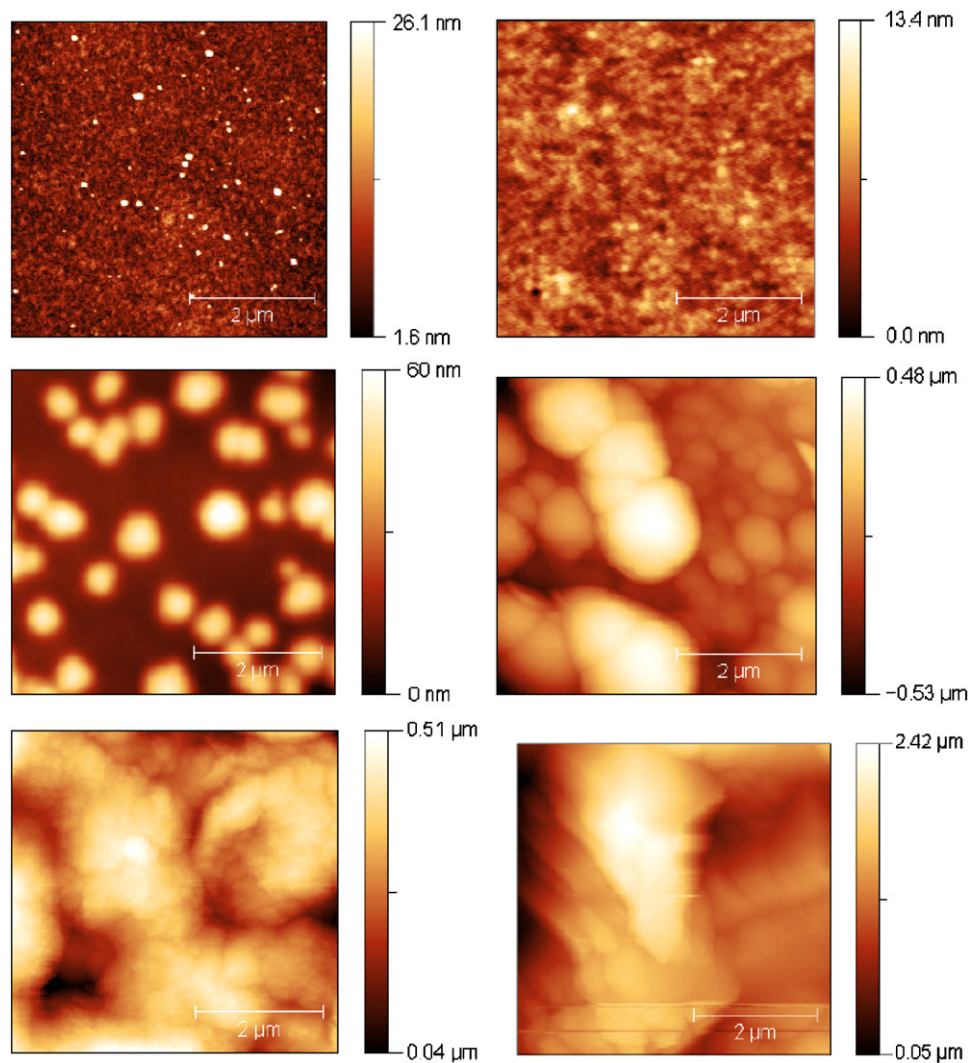


**Fig. 7.** AFM images (measuring  $5 \times 5 \mu\text{m}^2$ ) of the individual surfaces of the device. The PET substrate surface (top left) and the ITO surface (top right) are very smooth with a range of heights of 0–30 nm. The knife-over-edge-coated zinc oxide nanoparticle film is slightly rougher, presenting a range of heights of 0–60 nm with distinct particles responsible for the height variations (middle left). The P3CT-ZnO (middle right) and PEDOT:PSS (bottom left) electrodes are both quite rough with heights in the range of 0–500 nm and grain-like structure. The silver (bottom right) has a very rough surface as expected with heights in the range 0–2500 nm due to the silver grains in silver paste.

particles which could be collapsed ZnO aggregates with heights of around 60 nm and a diameter of 300–500 nm [13].

The P3CT–ZnO layer was increasingly rough with variations in height in the range of 0–500 nm over the  $5 \times 5 \mu\text{m}^2$  area that was analysed. This roughness is comparable to the roughness obtained by spin coating a similar ink mixture as shown in a pad-printing study (this issue). The slot-die-coated film is thus comparable to spin-coated films in terms of smoothness of the surface. The PEDOT:PSS layer was increasingly rough, which is possibly related to the screen-printing mask. The silver electrode presented a very rough surface as is expected from the silver grains in the paste.

### 3.5. Module performance

The completed modules (Fig. 8) were flexible and quite robust. It was possible to cut them into shorter pieces without destroying the function of the devices by use of a simple knife or a sharp pair of scissors. It was also possible to laminate them between two sheets of PET, which offered some mechanical protection of the devices. The only important point to note is that very small bending radii should be avoided when flexing (or cutting) the modules.

For this work more than 150 m of PET/ITO material was employed for developing the inks and methods. About 550 PET/ITO modules were coated. The practical yield of final devices was around 350 modules of which around 150 were technically functional. In the case of devices where KOE-coated zinc oxide was used the open-circuit voltage for the individual cells was always around 100 mV (as much as 150 mV was observed in some cases for single cell/line). This evened out for the serially connected modules. The typical performance in device current for the modules is shown in Fig. 9.

In the case of modules prepared using a slot-die-coated ZnO-np layer the performance was significantly better. This is ascribed to the possibility to process a thicker ZnO layer using slot-die coating. In principle it should be possible to process the same layer thickness using both KOE and slot-die coating but since the KOE coating is more open to the atmosphere this proved problematic. It is assumed that higher open-circuit voltages should be reachable using KOE coating if the ZnO-np solutions could be stabilised better. There is still some development needed before the performance reaches that of optimised laboratory devices. The open-circuit voltage must be especially improved. In the case of slot-die coating of ZnO layers the achieved performance was significantly better.



Fig. 8. Photograph of one of the final modules in front of the R2R coater.

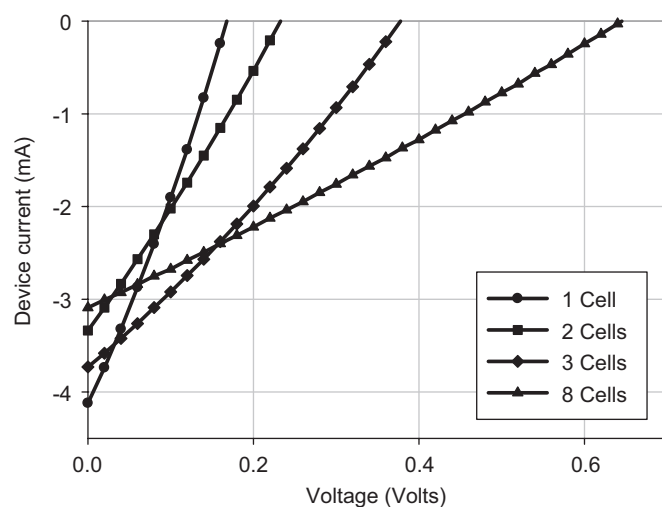


Fig. 9.  $I$ - $V$  curves for the four different devices (one-stripe, two-stripe, three-stripe and eight-stripe) prepared with a knife-over-edge-coated zinc oxide nanoparticle layer. The incident light intensity and temperature of the device were  $1000 \text{ W m}^{-2}$ , AM1.5G and  $72 \pm 2^\circ \text{C}$ , respectively.

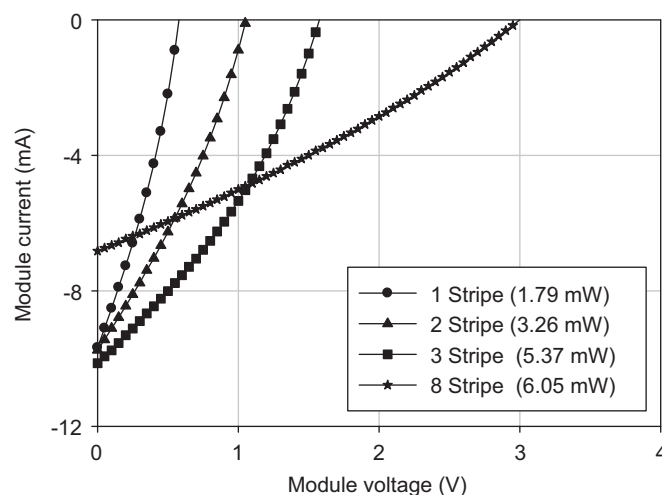


Fig. 10.  $I$ - $V$  curves for the modules prepared by slot-die coating the ZnO nanoparticle layer. The incident light intensity and temperature of the device were  $1000 \text{ W m}^{-2}$ , AM1.5G and  $72 \pm 2^\circ \text{C}$ , respectively. The output power at the maximum power point is shown in the inset.

The typical performance of the modules is shown in Fig. 10 for one-, two-, three- and eight-stripe modules. The voltage of each stripe was increased to around 500 mV and the current was more than doubled. The P3CT/ZnO bulk heterojunction has been shown to give a PCE of 0.2% ( $1000 \text{ W m}^{-2}$  AM1.5G,  $72 \pm 2^\circ \text{C}$ ) for devices with an active area of  $1 \text{ cm}^2$  using the same geometry as employed here (ITO/ZnO/P3CT–ZnO/PEDOT:PSS/silver) but on rigid glass substrates with very-high-conductivity ITO ( $< 10 \Omega \text{ square}^{-1}$ ). The lower voltage observed here is ascribed to problems with proper control of the quality of the ZnO layer. The current density reached in the model study was on the order of  $1 \text{ mA cm}^{-2}$  whereas the current density obtained here was in the range of  $0.4$ – $0.6 \text{ mA cm}^{-2}$ . The attraction of the P3CT/ZnO devices is that they are stable in air on storage and relatively stable during operation. This has enabled mass production of modules entirely by screen printing all layers in the device and allowed for public demonstration of the technology [3]. The performance of the devices in that study was quite low for modules comprising five serially

**Table 2**

Typical performance of the modules prepared by slot-die coating as shown in Fig. 10.

Module	Volts (V)	Current (mA)	FF (%)	Max. power (mW)	Module PCE (%)	Active area PCE (%)
1 stripe	0.58	9.67	31	1.79	0.031	0.12
2 stripe	1.06	9.75	31	3.26	0.037	0.11
3 stripe	1.58	10.13	33	5.37	0.046	0.12
8 stripe	2.99	6.82	29	6.05	0.023	0.05
8 stripe <sup>a</sup>	3.69	85.74	31	100.5	0.375	0.84

The nominal active area of each stripe is 15 cm<sup>2</sup>. The measurement conditions were 1000 W m<sup>-2</sup>, AM1.5G, 72 ± 2 °C. The values are for the module.

<sup>a</sup> Performance of a P3HT-PCBM module processed entirely from solution using slot-die coating.

connected cells in a concentric arrangement. The total module area in that case was 133 cm<sup>2</sup> with an active area of 75 cm<sup>2</sup>. The corresponding module efficiency and active area efficiency in that case were, respectively, 0.0075% (module) and 0.013% (active area). The geometric fill factor was 56% and the typical module output power was 1 mW. In the case of the modules prepared here the active area performance was significantly improved as summarized in Table 2 for the devices shown in Fig. 10. The improvement in performance is by a factor of ~10 on the active area and a factor of ~6 on the module. The performance obtained here on the active area is about 60% of the laboratory module results. For silicon solar cells, mass-produced devices typically yield a performance of 50–70% of the laboratory cells (known as champion or hero cells) [18]. While the performance is admittedly poor the improvement that has been reached by changing the film-forming technique is significant.

### 3.6. Comparison with P3HT-PCBM devices

The motivation for using the P3CT-ZnO technology as described above has its roots in the fact that the first public demonstration and free distribution of polymer solar cells was based on this technology [3]. To be fair a comparison with the state of the art in polymer photovoltaics was made to balance the view. The advantages of the thermocleavable materials and ZnO are stability and processing that allows for a switch between the soluble P3MHOCT and the insoluble P3CT. In the context of multilayer processing it is problematic to process subsequent layers if the underlying layers are soluble in the solvents employed in later steps. This is particularly challenging with P3HT-PCBM, which are both relatively soluble materials. To be fair the same processing methods were employed here, i.e. all-solution processing and no vacuum steps. It was found by processing a relatively thick P3HT-PCBM layer of 500 nm, a relatively thick PEDOT:PSS layer (250 nm) and fast drying of the silver back electrode that it was possible to obtain functional modules that outperform the P3CT-ZnO devices by a significant margin as shown in Fig. 11. By slot-die coating the silver electrode at relatively high coating speed of up to 1 m min<sup>-1</sup> it was possible to reduce the time between coating and drying to around 30 s and obtain functional modules. It was not possible to obtain functional modules by screen printing the PEDOT:PSS layer followed by screen printing the silver electrode on P3HT-PCBM devices. It should be stressed that slot-die coating of a thinned Dupont 5007 is not viewed as an optimal silver back electrode and it is reasonable to assume that the performance can be improved even further by seeking alternative silver formulations or alternative coating methods.

The performance of the eight-stripe P3HT-PCBM module shown in Fig. 11 has also been included in Table 2 and presents 100 mW output power with an active area PCE of 0.84%. The performance of P3HT-PCBM is thus 10 times better

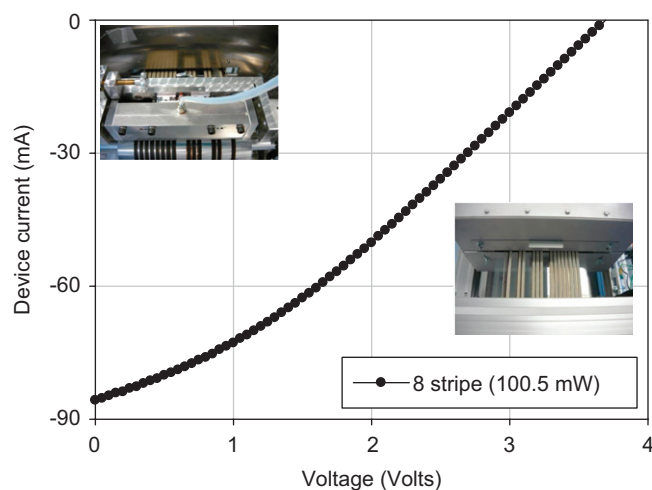


**Fig. 11.** I-V curve for the eight-stripe module based on P3HT-PCBM prepared entirely by slot-die coating the ZnO nanoparticle layer, the active layer, the PEDOT:PSS layer and the silver back electrode. The incident light intensity and temperature of the device were 1000 W m<sup>-2</sup>, AM1.5G and 72 ± 2 °C, respectively. The insets show slot-die coating of the silver electrode (left photograph) and the web with dried silver electrodes as it exits the drier (right photograph).

than that of P3CT-ZnO under approximately the same processing conditions. It is possible that the performance of P3HT-PCBM can be improved by judicious choice of the silver formulation such that the active layer thickness can be decreased to 200–300 nm and the thickness of the PEDOT:PSS can be decreased also. The large thicknesses employed here were necessary for device function. Thinner layers gave devices with short circuit. P3HT-PCBM has been reported by Plextronics to perform significantly better than shown here when prepared on rigid substrates [19].

### 3.7. Future work

A clear limitation in terms of materials is that ITO is employed as the transparent conductor. This has at least two implications; firstly the ITO is applied onto the PET substrate by sputtering (a vacuum process) and the use of ITO is undesirable due to its cost. A second limitation is the thermal properties of the PET substrate, which support temperatures only up to 140 °C. While thermocleavage is possible it takes several hours. If a temperature of 210 °C could be reached this would enable thermocleavage during R2R processing of the active layer. Future work should thus aim at alleviating the use of ITO as the transparent conductor such that modules can be prepared on a substrate that allows for processing at temperatures of at least 210 °C. In addition no vacuum steps should be involved at all.

#### 4. Conclusions

In this report I have detailed the transfer of the P3CT/ZnO technology to methods giving full R2R compatibility in the ambient atmosphere with no vacuum coating steps being involved during the processing of the five layers of the modules. All printing and coating techniques employed are fully R2R compatible while the last two layers of the device had to be prepared using sheet-fed printing due to the thermal properties of the PET substrate, which do not allow for fast thermocleavage of P3MHOCT to P3CT. The technical yield was quite low and needs to be improved. The performance of the modules was improved significantly as compared to a previous example of large-scale preparation of serially connected modules using entirely screen printing as the film-forming technique. Finally a comparison with the state-of-the-art as represented by P3HT-PCBM was made.

#### Acknowledgements

This work was supported by the Danish Strategic Research Council (DSF 2104-05-0052 and 2104-07-0022). I would like to thank Jan Fyenbo at Mekoprint Electronics A/S for assisting with the processing of the PET-ITO substrate and Jan Alstrup for technical assistance.

#### References

- †A patent application covering these inventions has been filed.
- [1] F.C. Krebs, Fabrication and processing of polymer solar cells. A review of printing and coating techniques, *Sol. Energy Mater. Sol. Cells*, doi:10.1016/j.solmat.2008.10.004.
  - [2] F.C. Krebs, H. Spanggaard, T. Kjær, M. Biancardo, J. Alstrup, Large area plastic solar cell modules, *Mater. Sci. Eng. B* 138 (2007) 106–111.
  - [3] F.C. Krebs, M. Jørgensen, K. Norrman, O. Hagemann, J. Alstrup, T.D. Nielsen, J. Fyenbo, K. Larsen, J. Kristensen, A complete process for production of flexible large area polymer solar cells entirely using screen printing—first public demonstration, *Sol. Energy Mater. Sol. Cells* 93 (2009) 422–441.
  - [4] F.C. Krebs, Air stable polymer photovoltaics based on a process free from vacuum steps and fullerenes, *Sol. Energy Mater. Sol. Cells* 92 (2008) 715–726.
  - [5] T. Aernouts, P. Vanlaeke, W. Geens, J. Poortmans, P. Heremans, S. Borghs, R. Mertens, R. Andriessen, L. Leenders, Printable anodes for flexible organic solar cell modules, *Thin Solid Films* 451–452 (2004) 22–25.
  - [6] Marianne Strange, David Plackett, Martin Kaasgaard, Frederik C Krebs, Biodegradable polymer solar cells, *Sol. Energy Mater. Sol. Cells* 92 (2008) 805–813.
  - [7] J.Y. Kim, K. Lee, N.E. Coates, D. Moses, T.-Q. Nguyen, M. Dante, A.J. Heeger, Efficient tandem polymer solar cells fabricated by all-solution processing, *Science* 317 (2007) 222–225.
  - [8] E. Bundgaard, F.C. Krebs, Low band gap polymers for organic photovoltaics, *Sol. Energy Mater. Sol. Cells* 91 (2007) 954–985.
  - [9] S. Günes, H. Neugebauer, N.S. Sariciftci, Conjugated polymer-based organic solar cells, *Chem. Rev.* 107 (2007) 1324–1338.
  - [10] M. Jørgensen, K. Norrman, F.C. Krebs, Stability/degradation of polymer solar cells, *Sol. Energy Mater. Sol. Cells* 92 (2008) 686–714.
  - [11] H. Hoppe, N.S. Sariciftci, Morphology of polymer/fullerene bulk heterojunction solar cells, *J. Mater. Chem.* 16 (2006) 45–61.
  - [12] B.C. Thompson, J.M.J. Fréchet, Polymer–fullerene composite solar cells, *Angew. Chem. Intl. Ed.* 47 (2008) 58–77.
  - [13] F.C. Krebs, Y. Thomann, R. Thomann, J.W. Andreasen, A simple nanostructured polymer/ZnO hybrid solar cell—preparation and operation in air, *Nanotechnology* 19 (2008) 424013.
  - [14] J.S. Liu, E.N. Kadnikova, Y.X. Liu, M.D. McGehee, J.M.J. Fréchet, Polythiophene containing thermally removable solubilizing groups enhances the interface and the performance of polymer–titania hybrid solar cells, *J. Am. Chem. Soc.* 126 (2004) 9486–9487.
  - [15] F.C. Krebs, M. Jørgensen, Decomposable vehicles in printing or coating compositions, filing date 13.04.2007, WO2007118850 A1.
  - [16] M. Jørgensen, O. Hagemann, J. Alstrup, F.C. Krebs, Thermo-cleavable solvents for printing of conjugated polymer: Application in polymer solar cells, *Sol. Energy Mater. Sol. Cells* 93 (2009) 413–421.
  - [17] R.D. McCullough, R.D. Lowe, M. Jayaraman, D.L. Anderson, Design synthesis and control of conducting polymer architectures—structurally homogenous poly(3-alkylthiophenes), *J. Org. Chem.* 58 (1993) 904–912.
  - [18] B. von Roedern, H.S. Ullal, The role of polycrystalline thin-film PV technologies in competitive PV module markets, in: Proceedings of the 33rd IEEE Photovoltaic Specialists Conference, 2008, NREL/CP-520-42494, pp. 1–4.
  - [19] R. Tipnis, J. Bernkopf, S. Jia, J. Krieg, S. Li, M. Storch, D. Laird, Large-area organic photovoltaic module—fabrication and performance, *Sol. Energy Mater. Sol. Cells*, doi:10.1016/j.solmat.2008.11.018.